

2. Hudson, A. Development of symmetry in plants. *Annu. Rev. Plant. Physiol. Mol. Biol.* **51**, 349–370 (2000).
3. Jackson, D., Veit, B. & Hake, S. Expression of maize *KNOTTED1* related homeobox genes in the shoot apical meristem predicts patterns of morphogenesis in the vegetative shoot. *Development* **120**, 405–413 (1994).
4. Barton, M. K. & Poethig, R. S. Formation of the shoot apical meristem in *Arabidopsis thaliana*—an analysis of development in the wild type and in the *shoot meristemless* mutant. *Development* **119**, 823–831 (1993).
5. Clark, S. E., Jacobsen, S. E., Levin, J. Z. & Meyerowitz, E. M. The *CLAVATA* and *SHOOT MERISTEMLESS* loci competitively regulate meristem activity in *Arabidopsis*. *Development* **122**, 1567–1575 (1996).
6. Vollbrecht, E., Reiser, L. & Hake, S. Shoot meristem size is dependent on inbred background and presence of the maize homeobox gene, *knotted1*. *Development* **127**, 3161–3172 (2000).
7. Reiser, L., Sanchez-Baracaldo, P. & Hake, S. Knots in the family tree: evolutionary relationships and functions of *knox* homeobox genes. *Plant Mol. Biol.* **42**, 151–166 (2000).
8. Sinha, N. R., Williams, R. E. & Hake, S. Overexpression of the maize homeobox gene, *KNOTTED-1*, causes a switch from determinate to indeterminate cell fates. *Genes Dev.* **7**, 787–795 (1993).
9. Chuck, G., Lincoln, C. & Hake, S. *Knatt1* induces lobed leaves with ectopic meristems when overexpressed in *Arabidopsis*. *Plant Cell* **8**, 1277–1289 (1996).
10. Waites, R., Selvadurai, H. R., Oliver, I. R. & Hudson, A. The *PHANTASTICA* gene encodes a MYB transcription factor involved in growth and dorsoventrality of lateral organs in *Antirrhinum*. *Cell* **93**, 779–789 (1998).
11. Timmermans, M. C., Hudson, A., Becraft, P. W. & Nelson, T. ROUGH SHEATH2: a Myb protein that represses *knox* homeobox genes in maize lateral organ primordia. *Science* **284**, 151–153 (1999).
12. Waites, R. & Hudson, A. *phantastica*: a gene required for dorsoventrality of leaves in *Antirrhinum majus*. *Development* **121**, 2143–2154 (1995).
13. Tsiantis, M., Schneeberger, R., Golz, J. F., Freeling, M. & Langdale, J. A. The maize *rough sheath2* gene and leaf development programs in monocot and dicot plants. *Science* **284**, 154–156 (1999).
14. Schneeberger, R., Tsiantis, M., Freeling, M. & Langdale, J. A. The *rough sheath2* gene negatively regulates homeobox gene expression during maize leaf development. *Development* **125**, 2857–2865 (1998).
15. Reidei, G. P. Non-mendelian megagametogenesis in *Arabidopsis*. *Genetics* **51**, 857–872 (1965).
16. Reinholz, E. *Arabidopsis thaliana* (L.) HEYNH. als Objekt für genetische und entwicklungsphysiologische Untersuchungen. *Arabidopsis Inform. Service* **01S**, 24 (1965).
17. Long, J. A., Moan, E. L., Medford, J. I. & Barton, M. K. A member of the *KNOTTED* class of homeodomain proteins encoded by the *STM* gene of *Arabidopsis*. *Nature* **379**, 66–69 (1996).
18. Lincoln, C., Long, J., Yamaguchi, J., Serikawa, K. & Hake, S. A *knotted1*-like homeobox gene in *Arabidopsis* is expressed in the vegetative meristem and dramatically alters leaf morphology when overexpressed in transgenic plants. *Plant Cell* **6**, 1859–1876 (1994).
19. Dockx, J. *et al.* The homeobox gene *ATK1* of *Arabidopsis thaliana* is expressed in the shoot apex of the seedling and in flowers and inflorescence stems of mature plants. *Plant Mol. Biol.* **28**, 723–737 (1995).
20. Lin, X. *et al.* Sequence and analysis of chromosome 2 of the plant *Arabidopsis thaliana*. *Nature* **402**, 761–768 (1999).
21. Long, J. & Barton, M. K. Initiation of axillary and floral meristems in *Arabidopsis*. *Dev. Biol.* **218**, 341–353 (2000).
22. Endrizzi, K., Moussian, B., Haecker, A., Levin, J. Z. & Laux, T. The *SHOOT MERISTEMLESS* gene is required for maintenance of undifferentiated cells in *Arabidopsis* shoot and floral meristems and acts at a different regulatory level than the meristem genes *WUSCHEL* and *ZWILLE*. *Plant J.* **10**, 101–113 (1996).
23. Clark, S. E., Running, M. P. & Meyerowitz, E. M. *CLAVATA3* is a specific regulator of shoot and floral meristem development affecting the same processes as *CLAVATA1*. *Development* **121**, 2057–2067 (1995).
24. Mayer, K. F. *et al.* Role of *WUSCHEL* in regulating stem cell fate in the *Arabidopsis* shoot meristem. *Cell* **95**, 805–815 (1998).
25. Aida, M., Ishida, T. & Tasaka, M. Shoot apical meristem and cotyledon formation during *Arabidopsis* embryogenesis: interaction among the *CUP-SHAPED COTYLEDON* and *SHOOT MERISTEMLESS* genes. *Development* **126**, 1563–1570 (1999).
26. Sundaresan, V. *et al.* Patterns of gene action in plant development revealed by enhancer trap and gene trap transposable elements. *Gene Dev.* **9**, 1797–1810 (1995).
27. Li, J., Nagpal, P., Vitart, V., McMorris, T. C. & Chory, J. A role for brassinosteroids in light-dependent development of *Arabidopsis*. *Science* **272**, 398–401 (1996).
28. Springer, P. S., McCombie, W. R., Sundaresan, V. & Martienssen, R. A. Gene trap tagging of *PROLIFERA*, an essential *MCM2-3-5*-like gene in *Arabidopsis*. *Science* **268**, 877–880 (1995).
29. Hajdukiewicz, P., Svab, Z. & Maliga, P. The small, versatile pPZP family of *Agrobacterium* binary vectors for plant transformation. *Plant Mol. Biol.* **25**, 989–994 (1994).
30. Liu, Y. G., Mitsuikawa, N., Oosumi, T. & Whittier, R. F. Efficient isolation and mapping of *Arabidopsis thaliana* T-DNA insert junctions by thermal asymmetric intercalated PCR. *Plant J.* **8**, 457–463 (1995).

Acknowledgements

We thank A. Groover, C. Kidner, E. Vollbrecht, M. Timmermans, J. Golz and D. Jackson for helpful discussions, Q. Gu, P. Springer, J. Li and J. Chory for help with mapping and T. Laux for *wus-1* seed. We also thank T. Mulligan for plant care, and K. Schutz and D. McCombie for help with sequencing. This work was supported by a Human Frontiers Science Program postdoctoral fellowship to M.C., a Biotechnology and Biological Sciences Research Council studentship to R.B. and grant support from the National Science Foundation, Department of Energy and United States Department of Agriculture to R.M.

Correspondence and requests for materials should be addressed to R.M. (e-mail: martiens@cshl.org).

Neuronal switching of sensorimotor transformations for antisaccades

Mingsha Zhang & Shabtai Barash

Department of Neurobiology, Weizmann Institute of Science, Rehovot, Israel

The influence of cognitive context on orienting behaviour can be explored using the mixed memory-prosaccade, memory-anti-saccade task. A symbolic cue, such as the colour of a visual stimulus, instructs the subject to make a brief, rapid eye movement (a saccade) either towards the stimulus (prosaccade) or in the opposite direction (antisaccade)^{1–3}. Thus, the appropriate sensorimotor transformation must be switched on to execute the instructed task. Despite advances in our understanding of the neuronal processing of antisaccades^{4–8}, it remains unclear how the brain selects and computes the sensorimotor transformation leading to an antisaccade. Here we show that area LIP of the posterior parietal cortex is involved in these processes. LIP's population activity turns from the visual direction to the motor direction during memory-antisaccade trials. About one-third of the visual neurons in LIP produce a brisk, transient discharge in certain memory-antisaccade trials. We call this discharge 'paradoxical' because its timing is visual-like but its direction is motor. The paradoxical discharge shows, first, that switching occurs already at the level of visual cells, as previously proposed by Schlag-Rey and colleagues⁹; and second, that this switching is accomplished very rapidly, within 50 ms from the arrival of the visual signals in LIP.

Figure 1a illustrates the problem raised in ref. 5. At the core of the sensorimotor transformation guiding antisaccades lies vector inversion. How does the brain compute this inversion? Figure 1b sketches relevant processing at the single-cell level. Figure 1b refers to visual and motor activity; a standard criterion for distinguishing between visual and motor activity is by timing the activity in memory-saccades^{9–15}, as shown below. For brevity, we call cells with visual activity 'visual cells', and cells with motor activity 'motor cells'. Although Fig. 1b is simplistic, it provides a framework for the two hypotheses we will consider for task switching. Both hypotheses propose that prosaccades and antisaccades involve alternative sets of functional connections between cells. A standard set of connections leads to prosaccades. A different set of connections, that emerges during training, leads to antisaccades. An instruction to perform an antisaccade switches the set of active connections from one configuration to the other.

According to the "visual switching hypothesis" (proposed in ref. 5), the switched connections are between visual cells. The process of switching connections would be reflected in a critical set of visual cells, each having two alternative receptive fields, a standard receptive field for ordinary prosaccades and another receptive field in the opposite direction specifically for antisaccades. Activation of the new receptive field, through the new connections, would instigate vector inversion. Thus, vector inversion would be accomplished by receptive field remapping¹⁶. The "visuomotor switching hypothesis" proposes that switching acts on connections between visual and motor cells. The two hypotheses lead to contrasting experimental predictions with regard to each cell's visual receptive field (mapped relative to the visual vector) and motor field (mapped relative to the motor vector) in prosaccades and anti-saccades. The visuomotor switching hypothesis predicts that both visual and motor fields remain unchanged, in all cells. Although a critical set of cells with motor activity would fire in trials with opposite visual vectors in prosaccades and antisaccades, the motor fields of these cells would not change. In contrast, the visual switching hypothesis predicts changed receptive fields for some

visual cells. Therefore, at the outset of this study we considered the visuomotor hypothesis more likely.

We recorded neuronal activity from area LIP in two monkeys trained in memory-antisaccades and related tasks. When we isolated a cell, we determined its preferred direction by testing the cell's activity in memory-prosaccades made in 12 directions. We then studied the cell's activity with a mixed memory-prosaccade memory-antisaccade task (Fig. 1c). Because the instruction to make a prosaccade or an antisaccade is specified by the colour of the stimulus, which varies from trial to trial, the monkey can determine the movement direction appropriate for the current trial only upon stimulus presentation. Therefore, all sensorimotor transformation switching must follow stimulus onset.

The stimulus appeared in either of two opposite locations, always positioned so that one location fell in the cell's preferred direction and the other in the opposite direction. Thus, there were four types of trials, two prosaccades (V+M+ and V-M-) and two antisaccades (V+M- and V-M+). Here V+ and M+ signify that the visual stimulus, or the movement, respectively, are in the preferred direction, and V- and M- mean that they are opposite to the preferred direction⁶.

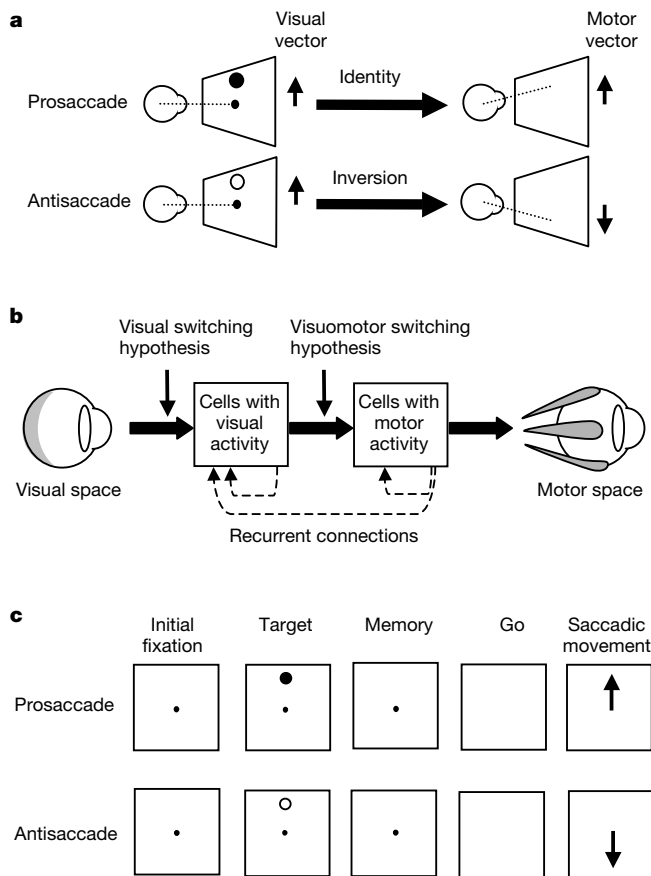


Figure 1 Cartoons of involved operations, hypotheses and task details. **a**, The sensorimotor transformations necessary for prosaccades and for antisaccades. The visual vector is defined as originating in the central fovea and terminating at the image of the visual stimulus. **b**, A cartoon showing sites where antisaccade-switching signals could act on the flow of information mediating ordinary saccades. Arrows should not be taken as literal direct connections; intermediates between visual and motor responses and multiple brain regions are involved. **c**, The task. The two types of trials differ only in the colour of the stimulus and the required movement (red stimulus signals a request for prosaccade, green for antisaccade). Typical durations are presaccadic fixation, 500 ms; stimulus, 250 ms; memory, 1,000 ms; postsaccadic fixation, 250 ms. To maintain movement precision in these conditions, at the end of some trials the stimulus reappeared and the monkey had to make a visually guided saccade to its location.

Figure 2a illustrates the activity of an LIP visual neuron. A brisk discharge briefly follows stimulus presentation in V+ trials, regardless of the subsequent saccade's direction (both V+M+ and V+M-). The discharge ends long before the movement. Therefore, this discharge is indeed visual, and is not motor. Moreover, the neuron remains almost inactive when visual stimuli are presented in the opposite direction (V- trials), regardless of saccade direction (V-M+ and V-M-). The activity of the cell illustrated in Fig. 2b is closely linked to the movement's planning and execution; for brevity we refer to such neurons as motor cells. Long after stimulus offset, a discharge builds up in M+ trials, gradually increasing towards the time of the saccadic movement (V+M+ and V-M+). The cell remains inactive in M- trials (V+M- and V-M-); hence this discharge is movement-related, or motor.

We computed for each neuron a 'differential activity' (DA) vector, mapping the neuron's activity in antisaccades onto the range between 'visual' and 'motor'. We define $DA(t) = R_{V-M+}(t) - R_{V+M-}(t)$ where $R_A(t)$ denotes the mean spike rate of the given neuron in trial group *A* at time *t* in the trial. We estimate the DA of a neuron as the bin-by-bin difference between the time-histograms of the two types of antisaccade trials, V-M+ and V+M-. Consistent with this definition, the visual neuron's DA is negative

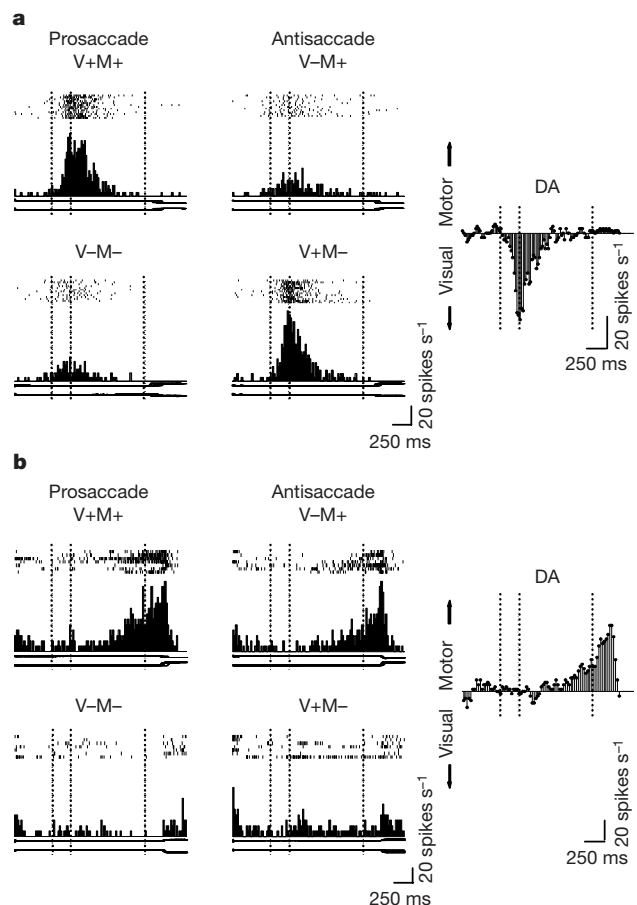


Figure 2 Responses of single PPC neurons. **a**, A visual cell and **b**, a motor cell. The four panels on the left of each part of the figure illustrate the neuron's response in trials of the types listed in the panel headers. Each panel contains, from the top, a raster illustrating spike timings, with each row showing a separate trial; a spike histogram (bin width 20 ms); and vertical and horizontal eye position traces. The panel on the right shows the differential activity vector (DA) of each cell. Time axis is the same for all panels. The scale of all four histograms of each part is shown on the left. Dashed vertical lines mark, from the left, onset and offset times of the stimulus and offset of the fixation spot (the 'go' signal). Thus, the stimulus is presented between the first two dashed vertical lines; the memory interval takes place between the second and third vertical lines.

throughout the trial (Fig. 2a) and the motor neuron's DA is positive throughout (Fig. 2b). We therefore call the negative direction of the DA 'visual' and the positive direction 'motor' (see Methods).

Figure 3 shows the mean DA of the full sample of 400 units that we studied, together with its pointwise 95% confidence interval. Soon after the onset of the visual stimulus (latency about 55 ms), the population DA turns towards the visual direction. The visual phase is brisk but brief: the peak of the visual phase is reached within another 100 ms. Afterwards the population DA rapidly declines and crosses over towards the motor direction. The population DA then gradually increases in the motor direction until the time of the saccadic movement, and only then goes down. Thus, the population DA has two clearly segregated phases, an early visual phase followed by a motor phase. The inversion from visual to motor occurs in the middle of the memory interval: by its pointwise 95% confidence interval, the zero crossing of the DA is between 140 and 690 ms (mean 415 ms) into the 1-s memory interval. The population DA thus provides a neuronal correlate of the transformation underlying antisaccade performance.

What events on the single-cell level trigger the inversion of the population activity? A novel type of discharge is illustrated by another LIP neuron (Fig. 4a). Three of the four conditions in Fig. 4a are consistent with the interpretation that this neuron is visual. Indeed, a visual response is evident in both V+ conditions (V+M+ and V+M-), as compared to the baseline condition (V-M-). However, this cell discharges vigorously also in the non-visual condition, V-M+. This discharge is paradoxical: although it is not visual, it appears to be visual in its time course. Its latency is brief, well within the range of visual response latencies¹²; and it declines to baseline during the memory period, long before the movement. Thus, the paradoxical activity differs markedly in its

time-course from the build-up activity of visuomotor and motor cells (Fig. 2b).

We analysed a set of 185 units selected to have strong visual response and little or no motor activity in memory-prosaccades, regardless of their activity in memory-antisaccades. This set

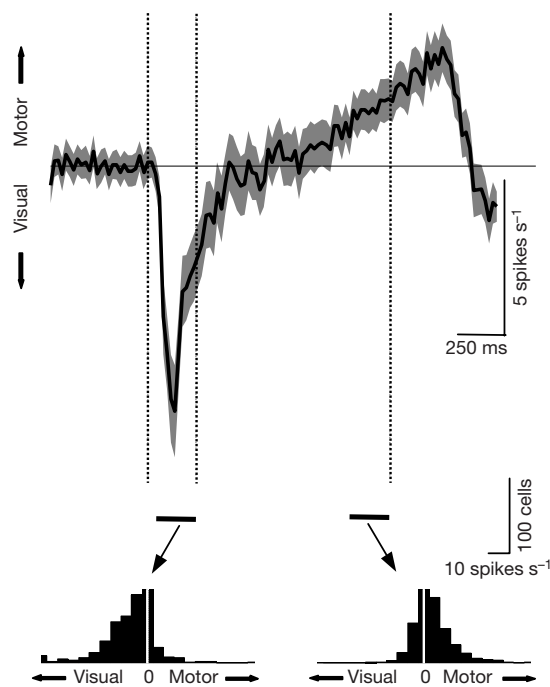


Figure 3 Mean differential activity for all 400 units studied. (Summed DA divided by number of units.) The DA is plotted in black. The pointwise 95% confidence interval, computed for each 20-ms bin, is shown in grey. Dashed vertical lines show, from the left, times of stimulus onset, stimulus offset and fixation spot offset, as in Fig. 2. The insets at the bottom show histograms of the mean DA computed for the two displayed 200-ms intervals, for each of the 400 units. The intervals span the visual response (50 to 250 ms after stimulus onset) and the last 200 ms of the memory interval. The histograms are clipped at 100 cells; actual values of the bins at 0 spikes per second are 132 and 163 cells for the left and right histograms, respectively.

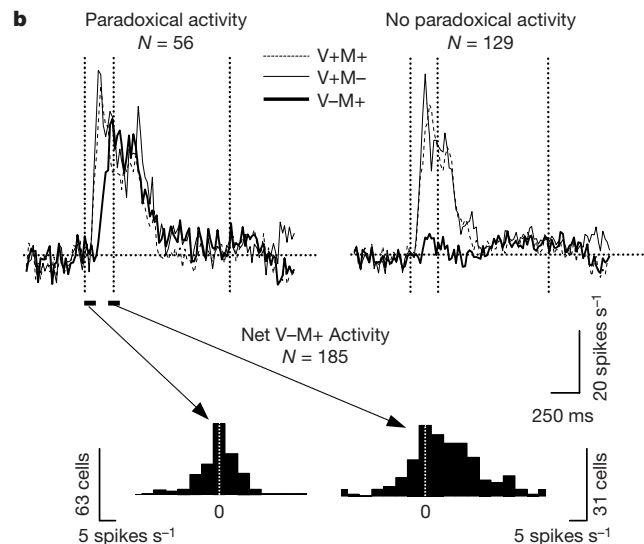
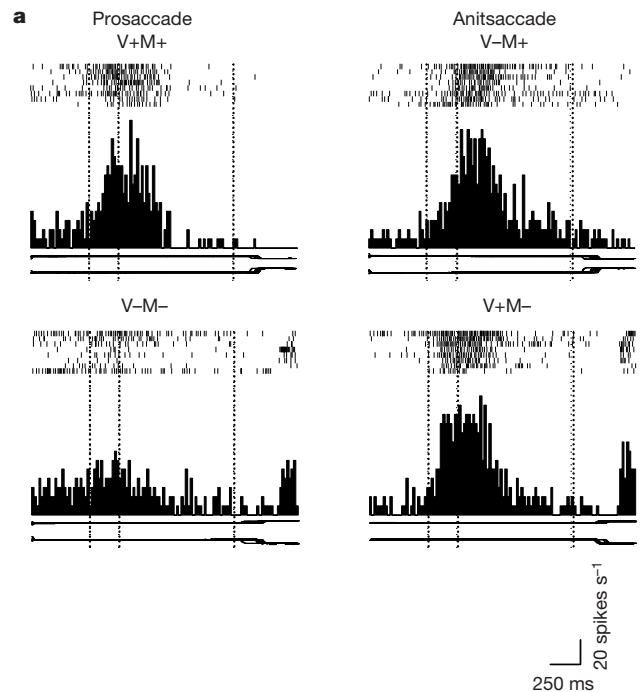


Figure 4 Illustration of the paradoxical activity. **a**, Activity of a visual cell with paradoxical activity, illustrated in the same format as in Fig. 2. **b**, Mean net responses in the paradoxical condition compared with the mean visual responses, for two complementary subsets of a set of 185 cells with visual activity but little or no motor activity. A net response is defined as the mean activity in the relevant condition minus the mean activity in the V-M-, baseline condition. The mean V-M+ response distinctly shows the paradoxical activity in the first group ($N = 56$, 30%) but is flat in the second group ($N = 129$, 70%). Vertical dashed lines have the same meaning as in Fig. 2. The insets at the bottom show histograms of the mean net activity in the V-M+ condition computed over 100-ms intervals before (left inset, 0 to 100 ms after stimulus onset) and during the paradoxical activity (right inset, 200 ms to 300 ms after stimulus onset). The histograms pull together data from both subsets displayed above. The mean of the left histogram is not significantly different from zero ($P = 0.78$); the mean of the second histogram, 5.53 spikes per second, is very significantly different from zero ($P = 0$ using standard double precision).

could be divided into two subsets, with ($N = 56, 30\%$) and without ($N = 129, 70\%$) substantial paradoxical activity. Figure 4b shows the mean net responses of these two groups. The net visual response in memory-prosaccades, $R_{V+M+}(t) - R_{V-M-}(t)$ is depicted as thin broken lines. The net visual response in memory-antisaccades, $R_{V+M-}(t) - R_{V-M-}(t)$ is depicted as thin solid lines. The non-visual condition, $R_{V-M+}(t) - R_{V-M-}(t)$ is depicted as thick solid lines. All four mean visual responses (thin lines) are similar. In contrast, the mean activity in the non-visual condition $V-M+$ (thick lines) shows a brisk discharge of paradoxical activity for the first group of cells, but remains at baseline for the second group. The latency of all four mean visual responses is about 60 ms. The latency of the mean paradoxical response is about 110 ms. Therefore, within 50 ms from the time of arrival of visual responses LIP is activated by input contingent on the task switch.

The presence of visual cells with paradoxical activity is consistent with the visual switching hypothesis (Fig. 1b). The paradoxical discharge might represent a remapped visual response to the oppositely directed stimulus, activated by nonstandard visual input connections. This nonstandard input pathway would usually be inactive. During the 110 ms after the onset of the visual stimulus, some context-categorization process switches these input connections on. After the 50-ms delay caused by context-categorization, the mean paradoxical activity increases rapidly, and then overlaps the mean visual response (Fig. 4b). This time course is consistent with the interpretation that the paradoxical activity is a visual response to the stimulus in the remapped receptive field.

Alternatively, the paradoxical activity might represent direct activation of the visual cell through its recurrent connections. According to this alternative interpretation, the cell's receptive field remains fixed. The paradoxical activity would reflect recurrent, top-down activation, rather than visual, bottom-up. Two waves would thus sweep through LIP shortly after stimulus presentation in antisaccade trials. Bottom-up visual responses, making up the first wave, would spread throughout the brain and feed into a context-categorization process. Within another 50 ms, the results of the context-categorization would reach LIP in the form of the second wave, consisting of the top-down paradoxical activity. Further experiments are needed to distinguish between these two interpretations. Furthermore, although the presence of the paradoxical activity shows that visual switching exists, it is still unclear whether visuomotor switching occurs too.

Our findings are consistent with Andersen's proposal in 1987 of posterior parietal cortex involvement in sensorimotor transformations¹⁷. Scalp recordings in humans performing anti-saccades support our findings¹⁸. A recent study of antisaccades in LIP⁶ addressed related but different questions and used substantially different procedures. It is possible that the late presaccadic signal described in ref. 6 is a variation of the paradoxical activity. The conclusions of ref. 6 were based mostly on saccades-on-demand; memory-saccades were made only in one direction, precluding direct comparison with our results. Finally, motor-intention dependent visual responses were recently described in the superior colliculus¹⁹, in another study, LIP auditory response fields were acquired by training²⁰. Perisaccadic receptive field remapping¹⁶ in some visual cells was also described in LIP. It remains to be seen whether the paradoxical activity has anything in common with these responses.

Thus, area LIP's population activity reflects the inversion transformation guiding antisaccades. About a third of LIP's visual cells show a novel type of discharge in antisaccade trials that is consistent with the visual switching hypothesis. The paradoxical activity might be a remapped visual response, or alternatively direct activation by recurrent connections. Task switching might also affect visuomotor connections. Altogether, our results reject the visuomotor connections as the sole site of switching, and therefore reject the visuomotor switching hypothesis. □

Methods

Two *Macaca fascicularis* monkeys were implanted with chronic-recording chambers placed over their posterior parietal lobules and scleral search coils for eye-position measurements. All techniques are standard. The experimental procedures conform to the US NIH guidelines and Israeli law and were approved by the Animal Care and Use Committee of the Weizmann Institute. According to standard physiological criteria^{11,12} the cells reported here were from area LIP. Nevertheless, a minority of the cells may have come from area MP²¹ or other neighbouring regions^{17,22}. The monkeys were first trained to perform memory-prosaccades with more than a second of memory, and only then to make memory-antisaccades. The task is illustrated in Fig. 1c. The red and green stimuli are isoluminant disks of the same size. The monkeys were also trained and tested in other oculomotor tasks. Some blocks contained the task of the present paper together with other conditions. We verified that these do not interact with the conditions described here by testing 12 cells with and without the additional conditions; the discharge characteristics remained unchanged. All recordings were conducted with the monkey in a completely darkened, sound-attenuated room. Fuller descriptions of the behavioural methods are given elsewhere²³. Following the isolation of a cell, we first mapped its preferred direction by testing the activity in memory-prosaccades made towards a target in one of 12 equally spaced locations on a 15° circle around a central fixation spot. Typical LIP cells have a clear preferred direction, and in visuomotor cells this direction is common to the visual, memory and motor discharges¹¹. All the cells in the present study had clear preferred directions, and were much less activated, if at all, in memory-prosaccades made in the opposite directions.

The DA represents the population vector

The DA approximates a given cell's net contribution to the population vector for antisaccades: The motor vectors produced in $V+M-$ and $V-M+$ trials are opposite in direction and equal in size. Therefore, the DA is a vector sum of the intended movement vectors weighted by the momentary spike rates: $DA(t) = R_{V+M-}(t)V_{V+M-} + R_{V-M+}(t)V_{V-M+}$ where V_A is the intended-movement vector of class A. This leads to the following interpretation of the DA. The preferred directions of LIP neurons are distributed roughly uniformly in all directions. Let us therefore assume, following ref. 24, that another LIP neuron could be matched to each neuron in our sample so that the temporal profile of the activity of that neuron would be identical to our neuron, but the preferred direction would be opposite. The net effect of the two neurons on the population vector would be $DA(t)$.

The paradoxical activity is not a visual response

The PPC is part of the dorsal visual stream and its neurons are known to be colour insensitive. Stimulus colour was used in previous PPC studies to indicate task context¹⁴. Nevertheless, we conducted a control study and tested the response of 26 visual neurons and another 8 visuomotor neurons in sequences of isoluminant red-blue-green-red, or red-green-green-red stimuli separated by memory intervals. The recordings were conducted long after the monkeys were overtrained in the task of Fig. 1c; the monkeys were easily trained to perform memory-prosaccades in response to these stimulus sequences. The differences between the responses to green and red in the control condition were negligible. All the neurons responded to a green stimulus in the opposite direction in a way similar to their response to a red stimulus in that location, in both cases much more weakly than to a stimulus of either colour in the receptive field. Therefore, the colour difference does not account for the paradoxical activity.

Received 22 May; accepted 19 September 2000.

- Hallett, P. E. Primary and secondary saccades to goals defined by instructions. *Vision Res.* **18**, 1279–1296 (1978).
- Amador, N., Schlag-Rey, M. & Schlag, J. Primate antisaccades. I. Behavioral characteristics. *J. Neurophysiol.* **80**, 1775–1786 (1998).
- Everling, S. & Fischer, B. The antisaccade: a review of basic research and clinical studies. *Neuropsychologia* **36**, 885–899 (1998).
- Funahashi, S., Chafee, M. V. & Goldman-Rakic, P. S. Prefrontal neuronal activity in rhesus monkeys performing a delayed anti-saccade task. *Nature* **365**, 753–756 (1993).
- Schlag-Rey, M., Amador, N., Sanchez, H. & Schlag, J. Antisaccade performance predicted by neuronal activity in the supplementary eye field. *Nature* **390**, 398–401 (1997).
- Gottlieb, J. & Goldberg, M. E. Activity of neurons in the lateral intraparietal area of the monkey during an antisaccade task. *Nature Neurosci.* **2**, 906–912 (1999).
- Everling, S., Dorris, M. C., Klein, R. M. & Munoz, D. P. Role of primate superior colliculus in preparation and execution of anti-saccades and pro-saccades. *J. Neurosci.* **19**, 2740–2754 (1999).
- Everling, S. & Munoz, D. P. Neuronal correlates for preparatory set associated with pro-saccades and anti-saccades in the primate frontal eye field. *J. Neurosci.* **20**, 387–400 (2000).
- Hikosaka, O. & Wurtz, R. H. Visual and oculomotor functions of monkey substantia nigra pars reticulata. III. Memory-contingent visual and saccade responses. *J. Neurophysiol.* **49**, 1268–1284 (1983).
- Gnadt, J. W. & Andersen, R. A. Memory related motor planning activity in posterior parietal cortex of macaque. *Exp. Brain Res.* **70**, 216–220 (1988).
- Barash, S., Bracewell, R. M., Fogassi, L., Gnadt, J. W. & Andersen, R. A. Saccade-related activity in the lateral intraparietal area. II. Spatial properties. *J. Neurophysiol.* **66**, 1109–1124 (1991).
- Barash, S., Bracewell, R. M., Fogassi, L., Gnadt, J. W. & Andersen, R. A. Saccade-related activity in the lateral intraparietal area. I. Temporal properties; comparison with area 7a. *J. Neurophysiol.* **66**, 1095–1108 (1991).
- Colby, C. L., Duhamel, J. R. & Goldberg, M. E. Visual, presaccadic, and cognitive activation of single neurons in monkey lateral intraparietal area. *J. Neurophysiol.* **76**, 2841–2852 (1996).
- Snyder, L. H., Batista, A. P. & Andersen, R. A. Coding of intention in the posterior parietal cortex. *Nature* **386**, 167–170 (1997).

15. Chafee, M. V. & Goldman-Rakic, P. S. Matching patterns of activity in primate prefrontal area 8a and parietal area 7ip neurons during a spatial working memory task. *J. Neurophysiol.* **79**, 2919–2940 (1998).
 16. Duhamel, J. R., Colby, C. L. & Goldberg, M. E. The updating of the representation of visual space in parietal cortex by intended eye movements. *Science* **255**, 90–92 (1992).
 17. Andersen, R. A. in *Handbook of Physiology, Section 1: The Nervous System* (eds Mountcastle, V. B., Plum, F. & Geiger, S. R.) 483–518 (Am. Physiol. Soc., Bethesda, 1987).
 18. Everling, S., Spantekow, A., Krappmann, P. & Flohr, H. Event-related potentials associated with correct and incorrect responses in a cued antisaccade task. *Exp. Brain Res.* **118**, 27–34 (1998).
 19. Horwitz, G. D. & Newsome, W. T. Separate signals for target selection and movement specification in the superior colliculus. *Science* **284**, 1158–1161 (1999).
 20. Grunewald, A., Linden, J. F. & Andersen, R. A. Responses to auditory stimuli in macaque lateral intraparietal area. I. Effects of training. *J. Neurophysiol.* **82**, 330–342 (1999).
 21. Thier, P. & Andersen, R. A. Electrical microstimulation distinguishes distinct saccade-related areas in the posterior parietal cortex. *J. Neurophysiol.* **80**, 1713–1735 (1998).
 22. Colby, C. L., Gattass, R., Olson, C. R. & Gross, C. G. Topographical organization of cortical afferents to extrastriate visual area PO in the macaque: a dual tracer study. *J. Comp. Neurol.* **269**, 392–413 (1988).
 23. Barash, S., Melikyan, A., Sivakov, A. & Tauber, M. Shift of visual fixation dependent on background illumination. *J. Neurophysiol.* **79**, 2766–2781 (1998).
 24. Newsome, W. T., Britten, K. H. & Movshon, J. A. Neuronal correlates of a perceptual decision. *Nature* **341**, 52–54 (1989).

Acknowledgements

We thank E. Ahissar for his involvement, and A. Melikyan and X. Wang for participation in some experiments. We thank M. Glickstein, P. Thier, E. Seidemann, Y. Ritov and M. Tsodyks for discussions and for reading the manuscript. This work was supported by the Israel Science Foundation, and by the Murray H. and Meyer Grodetsky Center for Research of Higher Brain Functions and the Einhorn-Dominic Institute of Brain Research at the Weizmann Institute, and by the Paul Godfrey Research Foundation.

Correspondence and requests for materials should be addressed to S.B. (e-mail: shabtai.barash@weizmann.ac.il).

A learning deficit related to age and β -amyloid plaques in a mouse model of Alzheimer's disease

Guiquan Chen*, Karen S. Chen†, Jane Knox*, Jennifer Inglis*, Andrew Bernard*, Stephen J. Martin*, Alan Justice†, Lisa McConlogue†, Dora Games†, Stephen B. Freedman† & Richard G. M. Morris*

* Department of Neuroscience, University of Edinburgh, 1 George Square, Edinburgh, EH8 9JZ, UK

† Elan Pharmaceuticals, 800 Gateway Boulevard, South San Francisco, California 94080, USA

Mice that overexpress the human mutant amyloid precursor protein (hAPP) show learning deficits, but the apparent lack of a relationship between these deficits and the progressive β -amyloid plaque formation that the hAPP mice display is puzzling. In the water maze¹, hAPP mice are impaired before and after amyloid plaque deposition^{2–7}. Here we show, using a new water-maze training protocol, that PDAPP mice⁸ also exhibit a separate age-related deficit in learning a series of spatial locations. This impairment correlates with β -amyloid plaque burden and is shown in both cross-sectional and longitudinal experimental designs. Cued navigation and object-recognition memory are normal. These findings indicate that A β overexpression and/or A β plaques are associated with disturbed cognitive function and, importantly, suggest that some but not all forms of learning and memory are suitable behavioural assays of the progressive cognitive deficits associated with Alzheimer's-disease-type pathologies.

We have developed a new water-maze protocol for mice in which, after they learn to escape quickly and reliably onto the hidden platform at one location, we move the platform to a new location. Numerous locations are used successively, one at a time. In such a procedure, earlier locations of the platform will be encoded in long-term memory, potentially causing interference. Memory retrieval must therefore be selective for the most recently encoded location,

an 'episodic-like' component of the task. The idea behind using such a procedure, embedded within a larger test battery, derives from lesion and single-unit recording studies in rodents that implicate the hippocampal formation in only certain aspects of spatial, working- or episodic-like memory^{9–13}. Such a protocol is worth exploring as, in the PDAPP mouse, the highest density of β -amyloid plaques is first seen in the outer molecular layer of the dentate gyrus and other regions of the hippocampus.

PDAPP and non-transgenic (non-Tg) littermate control mice ($n = 99$) swam normally and climbed successfully onto the escape

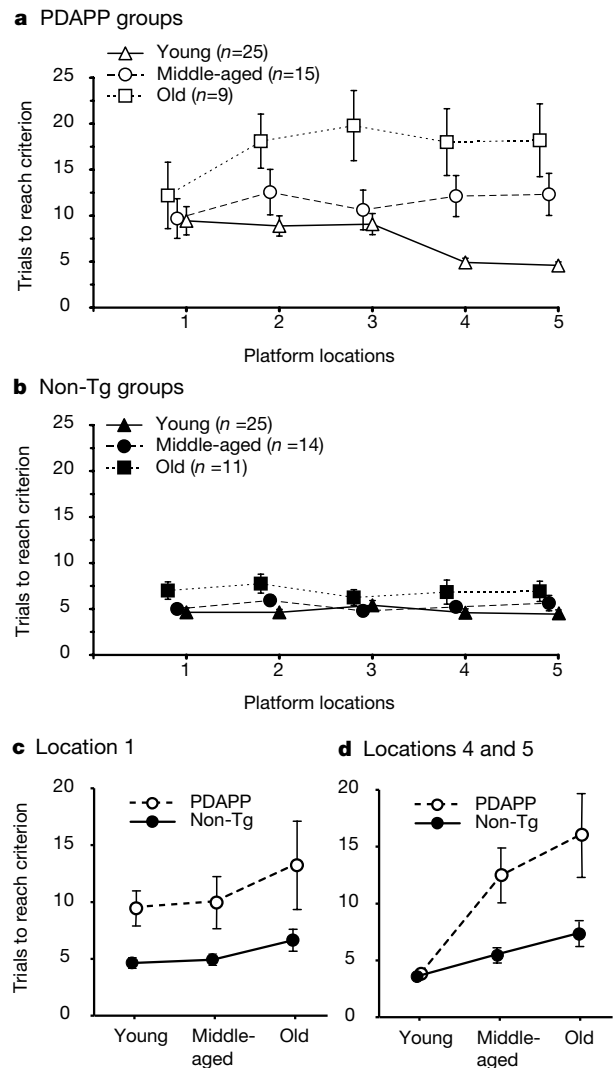


Figure 1 Age-related and age-independent deficits in spatial learning in PDAPP mice. Analysis of variance of 'trials to criterion' (3 successive trials with mean escape latency < 20 s) for each platform location of the first place navigation task revealed a significant groups \times age effect ($F = 5.27$, d.f. 2/93, $P < 0.01$). This interaction justified separate analyses of the two groups. **a**, PDAPP mice. Trials to criterion (inclusive) for each successive platform location in the main series of five locations revealed a significant age-related worsening of performance ($F = 8.32$, d.f. 2/46, $P = 0.001$) and a locations \times age interaction ($F = 2.17$, d.f. 6.59/151.7, $P < 0.05$; Greenhouse-Geisser correction). **b**, Non-Tg mice also showed a modest decline with age ($F = 7.24$, d.f. 2/47, $P < 0.005$) but no interaction. **c**, Platform location 1. A separate analysis of platform location 1 revealed poorer performance by the PDAPP mice which learned more slowly than non-Tgs ($F = 15.2$, d.f. 1/93, $P < 0.001$) but there was no age-related effect or interaction. **d**, Platform locations 4 and 5. There were significant main effects of group and age and, critically, a group \times age interaction ($F = 8.30$, d.f. 2/93, $P < 0.001$). This was because the PDAPP mice got worse with age ($F = 12.56$, d.f. 2/46, $P < 0.0005$) at a much faster rate than non-Tgs ($F = 4.45$, d.f. 2/47, $P < 0.05$). Results shown are mean \pm 1 s.e.m.